Journal of the European Ceramic Society **14** (1994) 303–311

Processing and Mechanical Properties of a Silicon Carbide Platelet/Alumina Matrix Composite

Y.-S. Chou & D. J. Green

Department of Materials Science and Engineering, The Pennsylvania State University, 509 Deike Bldg, University Park, PA 16802, USA

(Received 15 August 1993; accepted 11 January 1994)

Abstract

This paper presents an integrated study of the processing and mechanical properties of a SiC platelet/alumina composites. The major goal was to investigate the potential application of plate-like particles in toughening ceramic matrices. In the processing part of the study, the microstructures were found to possess preferred platelet orientation, with the platelets tending to lie parallel to each other after hot-pressing. In the mechanical property part of the study, Young's modulus, fracture toughness, flexural strength, and R-curve behavior were measured as a function of platelet content. It was determined that the preferred orientation did not lead to significant elastic anisotropy but it did lead to toughness anisotropy. Indeed the platelets led to a decrease in fracture toughness for crack propagating parallel to the platelet faces. In addition, it was found that the platelets also led to a strength decrease compared to the alumina. The optimum properties were a Young's modulus of 421 GPa, fracture toughness of 7·1 MPa√m, and a flexural strength of 480 MPa at SiC volume fraction of 0·3. Overall, it was concluded that with controlled processing SiC platelets are strong candidates for reinforcing ceramic matrices but that further development is needed.

In der vorliegenden Arbeit werden die Prozeß- und die mechanischen Eigenschaften von SiC-Lamellen/Aluminiumoxid-Verbunden untersucht. Das Hauptziel war, die möglichen Anwendungen von lamellenförmigen Teilchen zur Verstärkung von Keramiken zu ermitteln. Bei der Untersuchung des Herstellungsprozesses zeigte sich, daß das Gefüge überwiegend Lamellenorientierung besitzt, wobei die Lamellen nach dem Heißpressen vorzugsweise parallel zueinander liegen. Im zweiten Teil der Untersuchung wurden die mechanischen Eigenschaften wie Elastizitätzmodul, Bruchzähigkeit, Durchbiegefestigkeit und R-Kurvenverhalten als Funktion des Lamellenanteils bestimmt. Es zeigte sich, daß die vorzugsweise Orientierung der Lamellen nicht zu einer nennenswerten Anisotropie in der Elastizität führte, aber zu einem anisotropen Verhalten bezüglich der Zähigkeit. In der Tat hatten die Lamellen eine Verringerung der Bruchzähigkeit für Risse zur Folge, die parallel zu den Lamellen fortschritten. Außerdem ergab sich, daß die Lamellen zur Abnahme der Festigkeit, verglichen mit der von Aluminiumoxid, führte. Die optimalen Eigenschaften waren ein Elastizitätsmodul von 421 GPa, eine Bruchzähigkeit von 7·1 MPa√m und eine Durchbiegefestigkeit von 480 MPa bei einem SiC-Volumenanteil von 0·3. Zusammenfassend läßt sich schließen, daß sich SiC-Lamellen, hergestellt mit Hilfe eines kontrollierten Prozesses, als Verstärkung für Keramiken eignen, daß aber eine Weiterentwicklung des Prozesses notwendig ist.

Cette étude aborde simulatanément la fabrication et les propriétés mécaniques de composites plaquettes de SiC/alumine. Elle avait pour but principal d'évaluer dans quelle mesure des particules en forme de plaquettes peuvent améliorer la ténacité de matrices céramiques. La partie 'fabrication' montre qu'il y a une orientation préférentielle spontanée des plaquettes, celles-ci ayant tendance, lors du pressage à chaud, à s'aligner de telle sorte que leurs plans soient parallèles. L'étude mécanique comporte des mesures du module d'Young, de la ténacité, de resistance à la flexion, et de résistance à la propagation de fissures en fonction de la quantité de plaquettes. On montre que l'orientation préférentielle n'introduit pas d'anisotropie élastique, mais produit une anisotropie de la ténacité. Les plaquettes provoquent en effet une diminution de la résistance, comparée à celle de l'alumine. Les propriétés optimales sont: un module d'Young de 421 GPa, une ténacité

Journal of the European Ceramic Society 0955-2219/94/$7.00

de 7·1 MPa√m, une résistance à la flexion de 480 MPa, pour une fraction volumique de SiC de 0·3. Il semble en conclusion que, à condition d'être contrôlée, l'addition de plaquettes de SiC est une technique à considérer pour le renforcement de matrices céramiques; néanmoins une étude plus approfondie est nécessaire.

1 Introduction

Recent studies of whisker-reinforced ceramics have shown substantial improvements in fracture toughness and resistance to slow crack growth. For example, the fracture toughness, K_{Ic}, of alumina can be doubled or tripled to approximately 9·5 MPa√m with the addition of 30 vol.% SiC whiskers.[1,2] The creep rate of alumina at 1500°C can also be reduced to two orders of magnitude with a 15 wt% addition of whiskers.[3] Although whiskers have shown potential in improving the mechanical properties of ceramics, there still exist certain problems. For example, most commercially available whiskers have sizes in the submicrometer range, therefore they may present a health hazard when inhaled. In addition, the incorporation of rigid whiskers into a ceramic matrix constrains sintering and inhibits the densification process.[4–6] Due to their long, needle-like shape, whiskers are difficult to disperse and percolate the microstructure at low volume fractions.[7] As a result, whisker-reinforced composites require not only applied pressure but also much higher sintering temperatures for densification than the matrix alone.[2,8] A feasible solution to these problems is the replacement of whiskers with disc-shaped particles, e.g. SiC platelets. The larger dimensions of the available platelets present less of a health hazard than whiskers. In a two-dimensional arrangement, disc-shaped particles have a higher percolation threshold than whiskers and one would expect this to extend to three-dimensional arrays.[9] Preferred orientation of the platelets could also influence the percolation threshold but, of course, this could lead to significant anisotropy in the mechanical behavior. The substitution of platelets for whiskers, however, is primarily based on the assumption that the toughening mechanisms operating in whisker composites, e.g. bridging and crack deflection, could also occur in platelet composites and that similar strengths could be obtained.

To date, there are few papers discussing ceramic platelet composites. Sanders and Swain found that the addition of SiC platelets into an alumina matrix led to only ~30% increase in toughness, and the flexural strength decreased by a similar fraction from 550 MPa to ~380 MPa.[10] Claussen observed similar magnitude in toughness increase and strength decrease for SiC platelet/RBSN composites.[11] Nischik *et al.* studied the surface chemistry effect on the mechanical properties of SiC and Al_2O_3 platelet-reinforced composites.[12] The results showed that higher strength was obtained when using preoxidized SiC platelets but this led to a toughness decrease. Due to the very limited data about ceramic platelet composites, it is difficult to evaluate their potential in structural applications. The aim of this paper is to present data from an integrated study that considered the processing, microstructure, and mechanical behavior of a SiC platelet/alumina matrix composite.

2 Processing

2.1 Materials

The matrix phase in the composites was produced from a high-purity (>99·95%) α-alumina doped powder (Reynolds Metal Co., Reynolds High Purity Alumina, RC-HP DBM, Lot No. Bl-2596, AR) with 0·05 wt% MgO as a sintering additive. The major impurities in this powder are Na, Si, Fe and Ca with concentrations between 30 and 40 ppm. The mean particle size is 0·53 μm and the BET specific surface area is 8 m^2/g.

The reinforcing phase in the composites was α-SiC (c-axis, SiC platelet, SF-grade, Jonquiere, Canada) in the form of platelets. The crystal structure of the SiC platelets is hexagonal with 6H as the major phase and 4H as the minor. The major impurities are Al (0·7 wt%), Fe (0·02 wt%), and Ca (0·01 wt%).

Prior to mixing with the Al_2O_3 powder, the platelets were subjected to acid (≈0·18N HNO_3 solution) and base (≈0·15N NH_4OH solution) washes. Each wash lasted for 12 h. The purpose of these treatments was to remove leachable impurities (e.g. Al and Fe) and to improve the dispersion of the platelets in deionized water.[13]

2.2 Slip casting

Alumina slip was prepared by ball milling Al_2O_3 powders with deionized water in a 500 cm^3 plastic jar. The solid content of Al_2O_3 in the slip was 70 wt%. After milling for 24 h, the pH of the slurry was adjusted to 4·0 with nitric acid to maintain good dispersion.[13] The slip was allowed to sediment for 12 h to remove large particles. Silicon carbide platelets were then added into the slip such that composites with varying volume of platelets could be produced. Mixing was performed with a magnetic stirring rod. Finally, the slip was evacuated with a mechanical pump for several minutes before casting into square plates (50 × 50 × 5 mm).

2.3 Hot pressing

Densification of the green bodies was performed by hot pressing. The slip-cast samples were placed directly into a graphite die cavity and sintered under a vacuum of 0·2 Pa (10^{-4} torr) at 1650°C for 0·5 h. Pressure was gradually applied when the temperature reached 1400°C and maximum pressure (~25 MPa) was attained at 1650°C. The details of temperature and pressure profiles during hot pressing are shown in Fig. 1.

3 Characterization

3.1 Platelet diameter, thickness and aspect ratio

The diameter of the platelets was determined from micrographs by using an image analyzer (ZIDAS, Carl Zeiss Inc., Thornton, NY, USA). The diameter is defined to be the diameter of a circle having the same area as the platelets measured. The thickness of the platelets was directly measured from the micrographs. The aspect ratio, which is the ratio of diameter to thickness, was calculated using the average equivalent diameter and the mean thickness. Over two hundred platelets were measured.

3.2 Microstructure

The green density was calculated directly from the sample weight and dimensions. The sintered density was measured by the Archimedes displacement method. The theoretical densities for Al_2O_3 and SiC are 3·986 g/cm^3 and 3·22 g/cm^3, respectively. The theoretical density values for the composites were calculated by the rule of mixtures. Grain size of the Al_2O_3 was determined directly from the micrographs taken from thermally etched (1550°C, 15 min) samples. The SiC platelet orientation was determined by the Schulz reflection method using a pole-figure X-ray device.[14] Hot-pressed specimens with planes perpendicular to the pressing direction were ground parallel and polished with 6 μm diamond paste. Small square samples, with area of approximately 2·0 cm^2, were cut for measurement. The crystal plane chosen for X-ray analysis is (0006) of the 6H phase, which corresponds to the face of platelets. From the symmetry of the forming and densification procedures, one would expect the platelets to 'prefer' an orientation such that their faces are perpendicular to the hot-pressing direction. The details of the measurement of preferred orientation is available elsewhere.[15]

3.3 Mechanical properties

Young's modulus values were measured by the ultrasonic velocity method.[16] Due to the anisotropic microstructure, one would expect these materials to be transversely isotropic in their elastic behavior along two principal sample directions: one perpendicular and the other parallel to the hot-pressing axis. The specimen dimensions along both directions were about 3 mm. For each sample, three measurements were performed at different locations and the average values are reported.

Fracture toughness was measured by the indentation strength technique.[17] The impression was made on planes perpendicular and parallel to the hot-pressing axis as shown in Fig. 2 (marked A and B). The third possibility (case C) was not used due to sample size requirements, but was tested with another indentation method: direct crack measurement.[18] Beam samples (~40 × 3 × 3 mm) were aligned such that one set of the radial indentation cracks was parallel to the width direction. The impressions at locations A and B were made at an indent load of 98 N. Beams were then fractured with a screw-driven mechanical testing apparatus (Model 4212, Instron Corporation, Canton, MA, USA) in a four point bend test (outer span = 40 mm, inner span = 13·3 mm) at a crosshead speed of 0·5 mm/min. An averaged value of 4–5 specimens were reported for each volume fraction. From the fracture strength, σ_f,

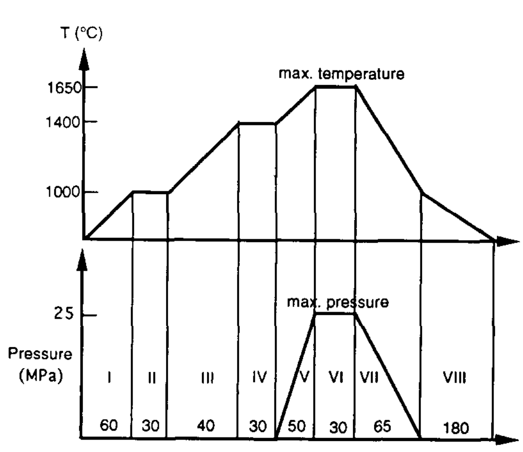

Fig. 1. Temperature and pressure profiles during hot-pressing.

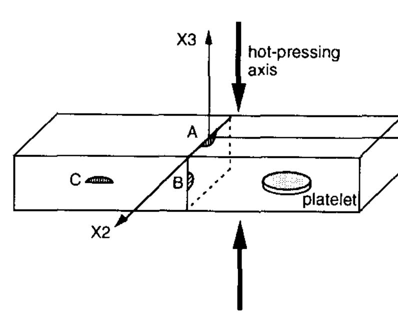

Fig. 2. Schematic of the indentation crack orientation used for toughness measurement. Only orientation A and B are used. Note that directions X2 and X3 are in the plane parallel to the hot-pressing axis (a perfectly oriented platelet is also shown).

and the indent load, P, the fracture toughness is calculated by eqn (1)[17]

$$K_C = \eta_V^R (E/H)^{1/8} (\sigma_f P^{1/3})^{3/4} \quad (1)$$

where E is Young's modulus, H is the hardness, and $\eta_V{}^R$ is a geometrical constant for which a value of 0·59 was used, as suggested in the literature.

The flexural strength of the composites was determined with a four-point bend test. The inner span was 10 mm and the outer span 20 mm. Test bars with dimensions of 25 × 3 × 3 mm were used. The sharp corners were beveled with diamond wheel (grit size 600) followed by 6 μm diamond paste polish. The test geometry was chosen such that the maximum tensile stress was applied in a direction on the plane perpendicular to the hot-pressing direction. For each batch, 4–5 samples were tested and the average values are reported.

To identify the microstructural effect on fracture toughness, a Vickers impression was made on well-polished surfaces with the trace of indentation crack propagating in three principal directions (Fig. 3): direction I is the crack propagating perpendicular to platelet faces, direction II perpendicular to platelet edges, and direction III parallel to platelet faces. In this method, the crack size was measured directly from the trace of the crack on the surface after each indentation. For the planes parallel to the hot-pressing axis, indentation was carefully made such that one set of the radial cracks were propagating perpendicular to platelet faces (direction I) and the other set parallel to the platelet faces (direction III). Once the crack size, c, as a function of load, P, was determined, the toughness data were calculated by eqn (2).[18]

$$K(c) = \S_V^R (E/H)^{0.5} (P/c^{1.5}) \quad (2)$$

where $\S_V^R$ is a material-independent constant for

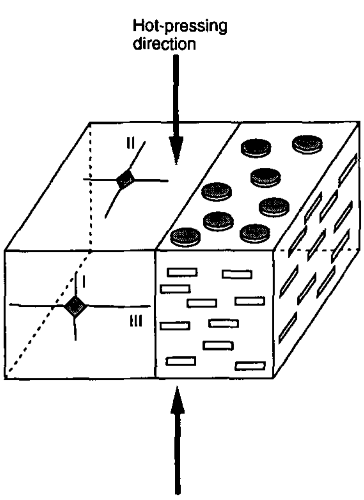

Fig. 3. Schematic of the directions for indentation crack length measurement. In directions I and II, the visible crack traces are propagating perpendicular to platelet edges and faces respectively, and in direction III the crack path is parallel to platelet faces.

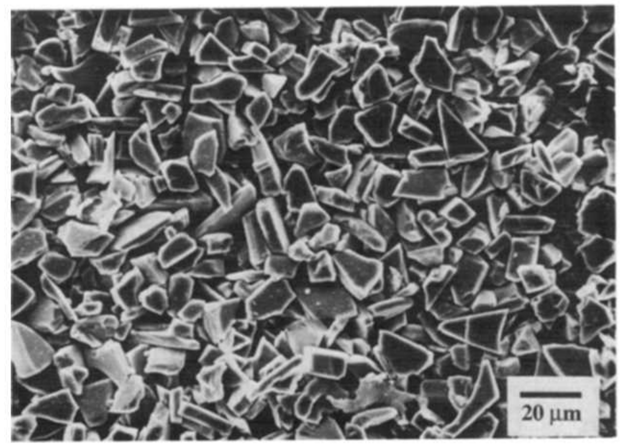

Fig. 4. SiC platelets used in this study.

Vickers-produced radial cracks. A value of 0·023 for $\S_V^R$ has been suggested by Ramachandran & Shetty in a study on R-curve behavior of toughened alumina ceramics.[19] By varying the indent load (4·9–294 N), the direct crack size measurement was used as an indication of whether there were any significant changes in fracture resistance with crack length in the composites (R-curve behavior). For each indent load, about 8–10 indentations were made and the average values are reported.

4 Results and Discussion

4.1 Characteristics of SiC platelets

Figure 4 shows the morphology of SiC platelets. It is clear that these platelets are not of any definite shape but are rather irregular. Therefore, the diameter of platelets was defined as the diameter of an equivalent circle with same area. The characteristics of SiC platelets, i.e. equivalent diameter, platelet thickness, and aspect ratio, are summarized in Table 1. It needs to be pointed out that the platelets were subjected to a sedimentation procedure to remove large and small platelets from the as-received powders. The size of the platelets for this study were rather small but were chosen because previous work had shown larger platelet sizes led to spontaneous microcracking.[20]

4.2 Green and hot-pressed density

In this study, slip casting was chosen as the forming technique based on the fact that high green density is often achieved with this method. High

Table 1. Characteristics of SiC platelets

Diameter (μm)		*Thickness (μm)*		*Aspect Ratio*	
Mean	*Range*	*Mean*	*Range*	*Mean*	*Range*
12	9–24	2	1–6	6	4–12

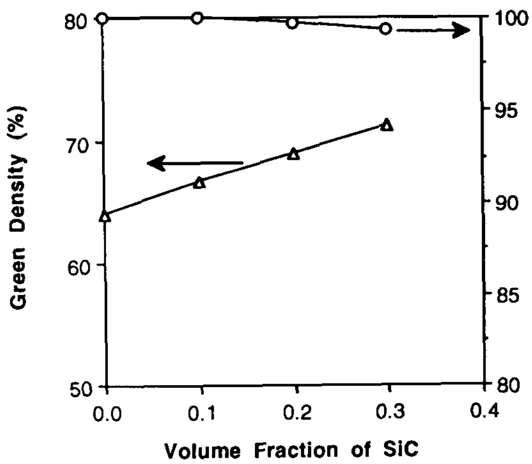

Fig. 5. Green and sintered density of SiC platelet/Al_2O_3 composites.

green density is expected to be beneficial in reducing the effect of constrained sintering during the densification process. The green and hot-pressed densities of the composites as a function of SiC volume fraction are shown in Fig. 5. It is clear that the green density increases with increasing SiC volume fractions. After hot pressing, all samples approached nearly full densification. Samples with high SiC loading shows a slight decrease in relative density; however, the porosity was less than 2% even at the highest SiC compositions.

It is worth noting that the hot-pressing temperature for whisker-reinforced composites is often much higher than those for platelet-reinforced composites. For example, the temperature is ≥1900°C for a 30 vol.% SiC whisker/Al_2O_3 composite to reach ≥98% of theoretical density,[1] whereas it is only 1650°C for the same loading of SiC platelet/Al_2O_3 composite.

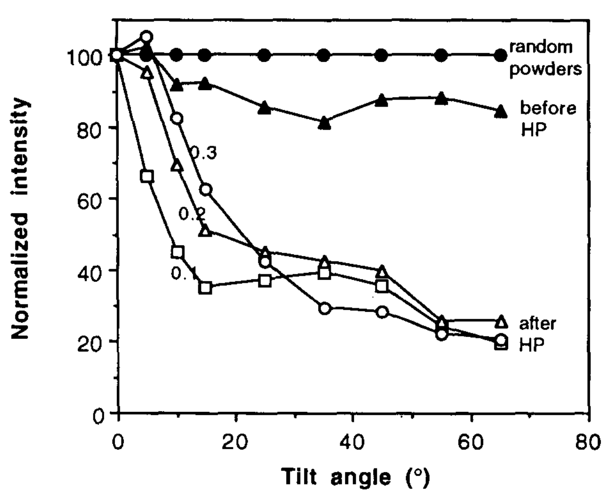

Fig. 6. Orientation distribution of SiC platelets in hot-pressed composites. Note that the platelet orientation in green bodies (▲) of a composite made with the same forming technique but with different source of SiC platelets is also shown (V_f = 0·15),[15] and the normalized intensity = $(I/I_{max})/(I/I_{max})_{random\ powder}$. Note that tilt angle = angle between the hot-pressing direction and the normal of the sample surface.

4.3 Preferred orientation

The orientation of SiC platelets in hot-pressed samples is shown in Fig. 6. For comparison, the platelet orientation in green bodies made with the same forming method is also plotted. It is clear that there exists a strong preferred platelet orientation after hot-pressing as compared with an ideal random orientation (shown by a horizontal line in Fig. 6). It also appears that composites with low SiC volume fraction tend to have stronger preferred orientation, for tilt angles less than 25°, than those with high volume fraction. The reason is not clear but it could be due to the physical interference between platelets that inhibits their rotation at higher volume fractions.

The preferred orientation was also confirmed by optical microscopy. Figure 7 shows the microstructures of the composites for planes perpendicular (Fig. 7(A)) and parallel (Fig. 7(B)) to the hot-pressing axis. It is clear that SiC platelets (white phase) tend to lie with their faces perpendicular to the hot-pressing axis. Preferred orientation is also found for whisker-reinforced composites after hot-pressing with the fiber axes being perpendicular to

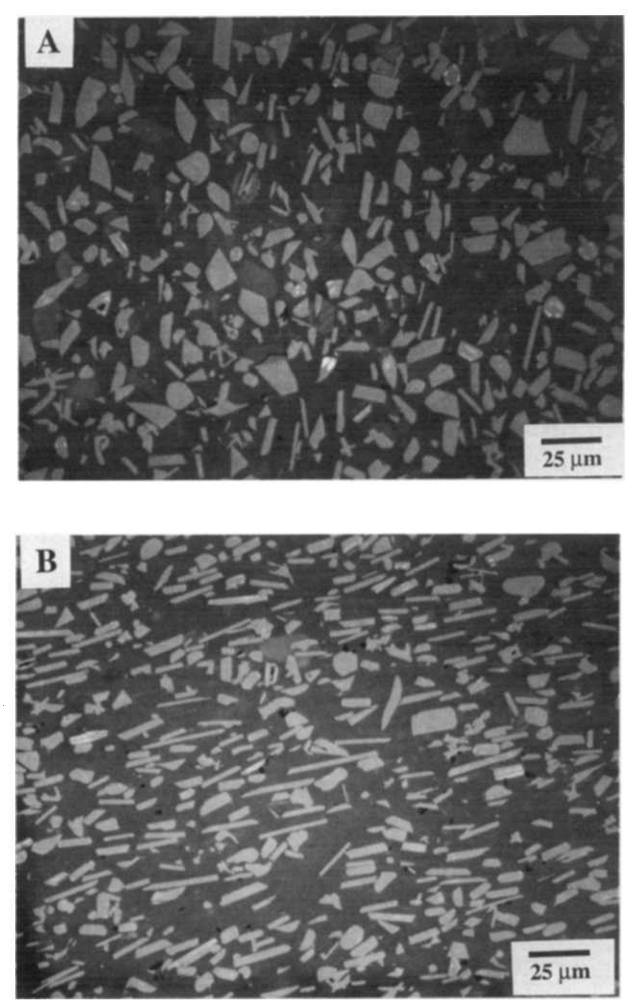

Fig. 7. Microstructure of hot-pressed composites. Optical micrographs were taken from planes (A) perpendicular and (B) parallel to the hot-pressing axis.

the hot-pressing direction. One would suspect, however, that the alignment of platelets should be easier than that of whiskers.

4.4 Young's modulus

Figure 8 shows the Young's moduli of the composites as a function of SiC volume fraction. Two principal directions are considered, one parallel and one perpendicular to the hot-pressing axis. It is apparent that the moduli increase continuously with SiC volume fraction for both directions. As the Young's modulus of dense alumina (around 380–408 GPa)[21–23] is just a little smaller than that of silicon carbide (around 420–450 GPa),[24,25] it is expected that the Young's modulus of the SiC/Al_2O_3 composite will increase slightly with increasing SiC volume fractions. As shown in Fig. 8, this behavior was confirmed.

It is also interesting to note that the moduli are slightly greater for parallel direction than those for perpendicular direction. This is due, in part, to the anisotropy in elastic stiffness for single-crystal α-SiC platelets. The elastic stiffness of hexagonal SiC along the crystallographic c axis, C_{33}, is 521 GPa, and is isotropic in the basal plane, $C_{11} = C_{22} = 479$ GPa.[26] Using these values one calculates Young's modulus values of 510 GPa and 455 GPa for these two principal directions respectively. It was shown in the previous section that there existed preferred orientation after hot-pressing and one would expect the modulus to be higher in the hot-pressing direction because the platelets tend to have their c axis oriented in this direction. However, as shown in Fig. 8, the difference in the elastic moduli is not substantial and one can assume that they are essentially isotropic.

4.5 Fracture toughness

The fracture toughness of SiC/Al_2O_3 composite as a function of SiC volume fraction is plotted in Fig. 9. The fracture toughness of composites

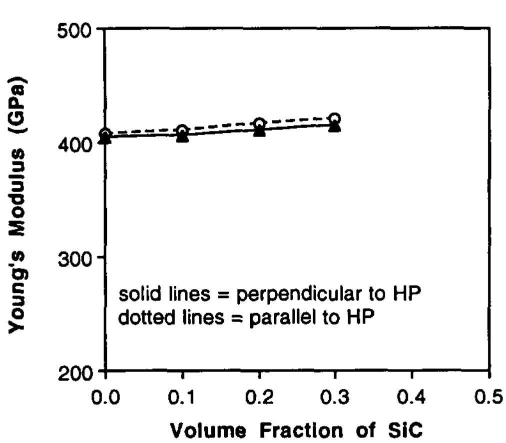

Fig. 8. Young's modulus of SiC/Al_2O_3 composites as a function of volume fraction of SiC platelets.

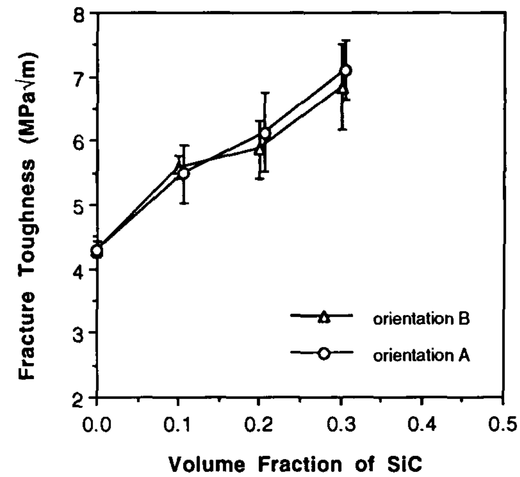

Fig. 9. Fracture toughness of SiC/Al_2O_3 composites as a function of volume fraction of SiC platelets.

increases continuously from 4·3 MPa√m ($V_f = 0{\cdot}0$) to 7·1 MPa√m ($V_f = 0{\cdot}3$) for the orientation A and to 6·7 MPa√m ($V_f = 0{\cdot}3$) for the orientation B. One would not expect significant toughness anisotropy for these orientations as both types of indentation cracks must interact with platelet faces and edges. For cracks running parallel to the platelet faces, one would expect only small changes in the fracture toughness as the cracks need not interact with the platelets at all. Indentation strength values for the fracture toughness of the orientation C were not obtained in the current study but some insight was obtained from the indentation crack length, to be discussed later.

For ceramic platelet composites, the incorporation of platelets into ceramic matrices has been found to increase the fracture toughness only to about 30% in previous studies.[10–12] In this study, the increase of toughness is approximately 70%, i.e. doubled, compared with other ceramic platelet composites. The current maximum toughness, 7·1 MPa√m, is lower than the reported value for whisker-reinforced composites, 9·5 MPa√m,[1] but it is felt that further improvements in processing to increase stronger degrees of preferred orientation and in platelet quality could allow higher toughness values to be obtained. The details of the toughening mechanisms in this system are discussed in Ref. 20 and it was concluded crack deflection by the platelets was the primary mechanism.

4.6 Toughness anisotropy

Considering the microstructure depicted in Fig. 3, one may expect that there could be three different toughness values when cracks are propagating along directions I, II and III. For two-dimensional cracks, the crack tip could be running (through thickness) perpendicular to the platelet faces (I), perpendicular to the platelet edges (II) or parallel

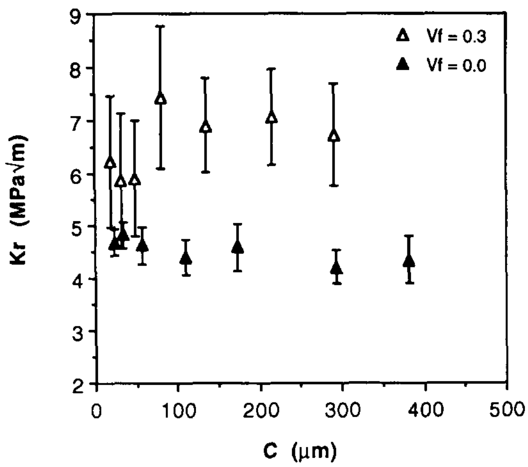

Fig. 10. Critical stress intensity factor versus indentation crack size for composites (V_f = 0·3) and alumina along crack direction I.

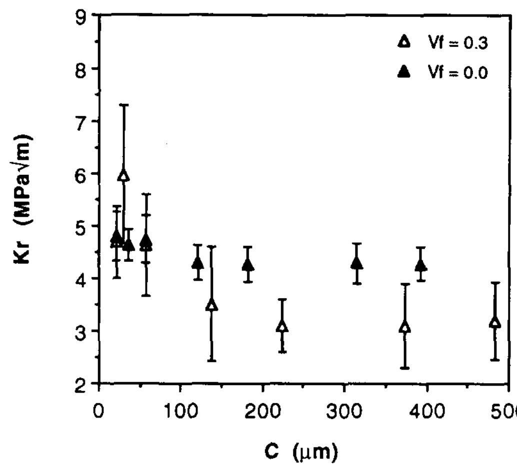

Fig. 12. Critical stress intensity factor versus indentation crack size for composites (V_f = 0·3) and alumina along crack direction III.

to the platelet faces (III). For indentation cracks, however, the situation is more complex as for orientations A and B (Fig. 2). The cracks must travel in both directions X2 and X3. It is, however, possible from indentation crack lengths to explore the toughness anisotropy, as one is usually measuring the trace of the crack that has propagated in a particular direction. This procedure does lead to some uncertainty, however, in that variation in fracture toughness in their plane could influence crack shape and hence the basis of the theoretical analysis.

Composites (V_f = 0·3) were indented (4·9–294 N) on different surfaces to determine toughness values along directions I, II and III. The results are shown in Figs 10–12 for directions I–III, respectively. For comparison, the data for hot-pressed plain alumina are also shown. It is clear that, considering the data fluctuation, there is no distinct difference for fracture toughness along directions I and II. In addition, the mean toughness values are in good agreement with the values in Fig. 9 for these two directions. There is, however, a substantial difference of direction III from the other two directions. The toughness values of direction III at higher indent loads (≥49 N, crack size ≥135 μm) are about half of those for the other directions. Moreover, they are even less than the alumina materials. This effect is probably due to high residual tensile stresses in this direction that result from the thermal expansion mismatch between the platelets and the alumina.[27] Similar results of toughness anisotropy for hot-pressed SiC_w(25 wt%)/Al_2O_3 composites were also reported, e.g., K_c = 5·30, 3·15 and 2·52 MPa√m for directions I, II and III, respectively.[28] Thus, one must bear in mind that there exists some compromise when one is increasing the toughness by using preferred orientation of the 'toughening' phase.

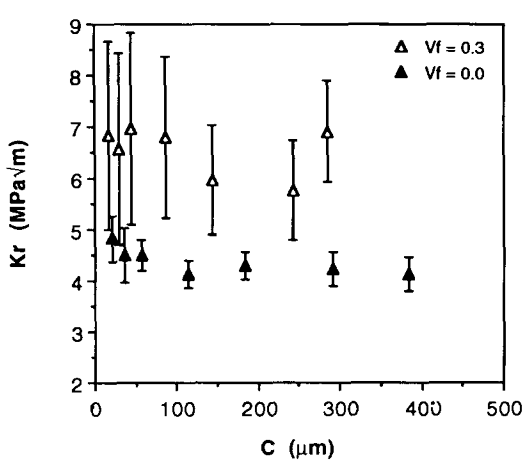

Fig. 11. Critical stress intensity factor versus indentation crack size for composites (V_f = 0·3) and alumina along crack direction II.

The data in Figs 10–12 can also be interpreted in terms of an *R*-curve, as one would expect increasing K_r values if there is a rising *R*-curve. No obvious increase was observed and further experiments confirmed there was no significant *R*-curve behavior in these materials.

4.7 Flexural strength

To reduce the effect of large machining flaws, composite samples were carefully polished with 6 μm diamond paste. The flexural strength of the composites as a function of SiC volume fraction is plotted in Fig. 13. Upon first addition of SiC platelets into the alumina matrix the flexural strength was greatly reduced from 610 MPa (V_f = 0) to 420 MPa (V_f = 0·1). The strength then reached a plateau value approximately 480 MPa at higher volume fractions. The decrease in flexural strength is most likely to be due to the presence of the platelets. From fracture surface analysis, large SiC platelets were identified as failure origins. Assuming internal circular cracks, the critical flaw radius (estimated from the toughness (Fig. 9) and the

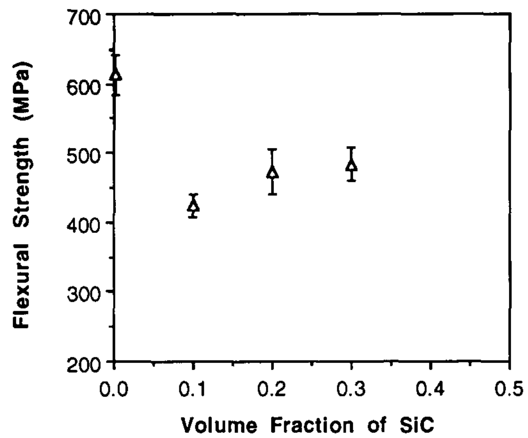

Fig. 13. Flexural strength of SiC/Al_2O_3 composites as a function of volume fraction of SiC platelets.

strength (Fig. 13) data) for alumina and the composites is ~30 μm and 110–140 μm, respectively. It is interesting to note that the critical flaw size of the composites is much larger than the platelet size (the platelet dimensions ranged from about 9 μm to 24 μm). The increase in critical flaw size may be due to the presence of the residual stress field which would promote stable crack growth in the composites. Further improvements in controlling platelet orientation such that all the platelets have the same orientation and using platelets with a narrower size distribution could be useful in minimizing the strength decrease. It is also worth noting that the flexural strength at higher volume fractions, e.g. 480 MPa (V_f = 0·3), is larger than lower volume fraction, e.g. 420 MPa (V_f = 0·1). This may be due to the higher toughness values at the higher volume fractions.

5 Summary and Conclusions

An in-depth study of the processing and mechanical properties of SiC platelet/Al_2O_3 composites was presented. From X-ray analysis and microscopy, the formation of preferred platelet orientation after hot-pressing was identified. There was some effect of SiC volume fraction on the preferred orientation; however, it was not substantial. The optimum mechanical properties of the composites were obtained with a SiC volume fraction of 0·3. These properties were a Young's modulus of 421 GPa, fracture toughness of 7·1 MPa$\sqrt{m}$, and a flexural strength of 480 MPa. There was strong anisotropy in fracture toughness as shown by the crack length measurements, in which cracks propagating parallel to the platelet faces encountered the least resistance. Overall, it appears that with controlled processing, SiC platelets/alumina composites are strong candidates for structural applications but there is a need for further work to find techniques to enhance the toughness values and to minimize the strength reduction.

Acknowledgement

This work was supported by the Cooperative Program at the Center for Advanced Materials, The Pennsylvania State University.

References

1. Homeny, J., Vaughn, W. L. & Ferber, M. K., Processing and mechanical properties of SiC-whisker–Al_2O_3-matrix composites. *Am. Ceram. Soc. Bull.*, **66** (1987) 333–8.
2. Tiegs, T. N. & Becher, P. F., Sintered Al_2O_3–SiC-whisker composites. *Am. Ceram. Soc. Bull.*, **66** (1987) 339–42.
3. Porter, J. R., Lange, F. F. & Chokshi, A. H., Processing and creep performance of SiC-whisker-reinforced Al_2O_3. *Am. Ceram. Soc. Bull.*, **66** (1987) 343–7.
4. Bordia, R. K. & Scherer, G. W., On constrained sintering–III. Rigid inclusions. *Acta Metall.*, **36** (1988) 2411–16.
5. Lange, F. F., Constrained network model for predicting densification behavior of composite powders. *J. Mater. Res.*, **2** (1987) 59–65.
6. Scherer, G. W., Sintering with rigid inclusions. *J. Am. Ceram. Soc.*, **70** (1987) 719–25.
7. Scher, H. & Zallen, R., Critical density in percolation processes. *J. Chem. Phys.*, **53** (1970) 3759–61.
8. Wei, G. C. & Becher, P. F., Development of SiC-whisker-reinforced ceramics. *Am. Ceram. Soc. Bull.*, **64** (1985) 298–304.
9. Holm, E. A. & Cima, M. J., Two-dimensional whisker percolation in ceramic matrix–ceramic whisker composites. *J. Am. Ceram. Soc.*, **72** (1989) 303–5.
10. Sanders, G. & Swain, M. V., Mechanical property and microstructural observations for some silicon carbide-reinforced alumina composites. *Materials Forum*, **14** (1990) 60–9.
11. Claussen, N., Ceramic platelet composites. In *11th RISO International Symposium on Metallurgy and Materials Science, Structural Ceramics Processing, Microstructure and Properties*, ed. J. J. Bentzen, J. B. Bilde-Sorensen, N. Christiansen, A. Horsewell & B. Ralph. 1990, pp. 1–12.
12. Nischik, C., Seibold, M. M., Travitzky, N. A. & Claussen, N., Effect of processing on mechanical properties of platelet-reinforced mullite composites. *J. Am. Ceram. Soc.*, **74** (1991) 2464–8.
13. Sacks, M. D., Lee, H.-W. & Rojas, O. E., Suspension processing of Al_2O_3/SiC whiskers composites. *J. Am. Ceram. Soc.*, **71** (1988) 370–9.
14. Schulz, L. G., A direct method of determining preferred orientation of a flat reflection sample using a geiger counter X-ray spectrometer. *J. Appl. Phys.*, **20** (1949) 1030–3.
15. Chou, Y.-S. & Green, D. J., SiC-platelet/Al_2O_3 composites, I. Effect of forming technique on platelet orientation. *J. Am. Ceram. Soc.*, **75** (1992) 3346–52.
16. Bhardwaj, M. C., Simple ultrasonic NDC for advanced ceramics development and manufacture. In *Advanced Metal and Ceramic Composites, Proceedings of International Conference on Advanced Metal & Ceramic Matrix Composites: P/M Processing, Process Modeling and Mechanical Behavior.* Anaheim, CA, 1990, pp. 1–15.
17. Chantikul, P., Anstis, G. R., Lawn, B. R. & Marshall, D. B., A critical evaluation of indentation techniques for measuring fracture toughness: II. Strength method. *J. Am. Ceram. Soc.*, **64** (1981) 539–43.

18. Anstis, G. R., Chantikul, P., Lawn, B. R. & Marshall, D. B., A critical evaluation of indentation techniques for measuring fracture toughness: I. direct crack measurements. *J. Am. Ceram. Soc.*, **64** (1981) 533–7.
19. Ramachandran, N. & Shetty, D. K., Rising crack growth-resistance (*R*-curve) behavior of toughened alumina and silicon nitride. *J. Am. Ceram. Soc.*, **74** (1991) 2634–41.
20. Chou, Y.-S., Processing and mechanical properties of SiC-platelet/Al_2O_3 composites. PhD Thesis, The Pennsylvania State University, PA, 1992.
21. Spriggs, R. M. & Vasilos, T., Effect of grain size and porosity on transverse bend strength and elastic modulus of hot-pressed alumina and magnesia. *Am. Ceram. Soc. Bull.*, **40** (1961) 187.
22. Soga, N. & Anderson, O. L., High-temperature elastic properties of polycrystalline MgO and Al_2O_3. *J. Am. Ceram. Soc.*, **49** (1966) 355–9.
23. Anderson, O. S., Schreiber, E., Liebermann, R. C. & Soga, N., Some elastic constant on minerals relevant to geophysics. *Rev. Geophys.*, **6** (1968) 491–524.
24. McMurphy, C. H., Kaspryzk, M. R. & Naum, R. G., In *Silicon Carbide 1973*. ed. R. C. Marshall, J. W. Faust, Jr & C. E. Ryan. University of South Carolina, SC, 1974, pp. 411–19.
25. Shaffer, P. T. B. & Jun, C. K., The elastic modulus of dense polycrystalline silicon carbide. *Mat. Res. Bull.*, **7** (1972) 63–70.
26. Li, Z. & Bradt, R. C., The single crystal elastic constants of hexagonal SiC to 1000°C. *Int. J. High Tech. Ceram.*, **4** (1988) 1–10.
27. Chou, Y.-S. & Green, D. J., SiC-platelet/Al_2O_3 composites, II. Mechanical properties. *J. Am. Ceram. Soc.*, **76** (1993) 1473–9.
28. Breder, K., Zeng, K. & Rowcliffe, J., Indentation testing of an Al_2O_3/SiC whisker composites. *Ceram. Eng. Sci. Proc.*, **10** (1989) 1005–13.